

# Copper clusters and small particles stabilized within nanoporous materials

V.S. Gurin<sup>1,a</sup>, V.P. Petranovskii<sup>2,b</sup>, A.N. Pestryakov<sup>3,4,c</sup>, A. Kryazhov<sup>4</sup>, O. Ozhereliev<sup>4</sup>, M.-A. Hernandez<sup>5</sup>, and A.A. Alexeenko<sup>6</sup>

<sup>1</sup> Physico-Chemical Research Institute, Belarusian State University, Minsk, Belarus

<sup>2</sup> CCMC-UNAM, Ensenada, Mexico

<sup>3</sup> Fritz Haber Institute, Department of Inorganic Chemistry, Berlin, Germany

<sup>4</sup> Tomsk Polytechnic University, Tomsk, Russia

<sup>5</sup> Institute of Sciences, University of Puebla, Puebla, Mexico

<sup>6</sup> Gomel State Technical University, Gomel, Belarus

Received 10 September 2002

Published online 3 July 2003 – © EDP Sciences, Società Italiana di Fisica, Springer-Verlag 2003

**Abstract.** Copper was incorporated into mordenites with variable  $\text{SiO}_2/\text{Al}_2\text{O}_3$  molar ratio, porous silica xerogels, natural pumice, and  $\gamma$ -alumina. The UV/Visible spectroscopy of the copper species produced as the result of hydrogen reduction and catalytic runs is presented. Different spectral features were detected assignable to nanoparticles, few-atomic clusters, oxide forms and Cu(II) compounds. The significant effect of support upon the redox-behavior of copper is discussed on the basis of experimental data.

**PACS.** 36.40.Vz Optical properties of clusters – 82.75.Vx Clusters in zeolites

## 1 Introduction

Ultrafine particles and clusters of metals dispersed within dielectric media provide various non-trivial features due to both own size-dependent properties and metal-support interaction [1–3]. These factors need to be controlled to attain desired properties of materials. The nature of a support is one of the most relevant factors influencing both physical and chemical characteristics of metal particles. Our previous studies of copper species (as well other transition metals) revealed that there are considerable changes in electronic and chemical properties of supported metals at the contact with supports with various acid-base features and porosity [4,5]. All these factors exert a direct effect on formation of active surface of metals and, accordingly, on their catalytic properties.

The paper joins several types of inorganic materials those allow size regulation of metal particles through a wide range: from few angstroms in the intracrystalline zeolite cavities (the lower-dimension pores) up to several microns within the higher dimension pores in silica and natural pumice. Zeolites have the uniform lower-dimension porous structure defined by long-order in crystals, while porous silica matrices and pumice possess variable pore dimensions regulated by preparation conditions and ther-

mal sintering. On the other hand, these materials contain both very narrow pores to incorporate molecular-dimension species and large pores. They can enclose metal clusters those do not exceed the geometrical dimensions of the cavities and incorporate nanoparticles of metal and metal compounds. Position of the particles is determined by the higher-dimension porosity. However, except of geometrical factor the formation of mono-size clusters can be conditioned by ionic properties of the matrices. These properties can be easily regulated in zeolites.

The great practical importance of metal on supports in catalysis provides necessity to study too complicated materials, however, some unique features of natural media may not be completely reproduced in more definite artificial ones. For example, copper in pumice composites are used for alcohol partial oxidation with the high yield, and the mechanism of this action remains not clear up to date [6]. Copper nanoparticles and clusters and partly charged  $\text{Cu}_n^{\delta+}$  clusters are active sites in these processes, and they are subjected a number of redox-transformations in catalytic systems [4,5,7].

In the present work, we summarize the selected results concerning optical properties of reduced copper metal clusters and nanoparticles supported in zeolites and the other porous matrices (silica xerogels, natural pumice and  $\gamma$ -alumina). These matrices are different in crystallinity and chemical composition, but they are similar in the significance of porosity into ability to incorporate metal ions and particles, and also in the nature of metal atom

<sup>a</sup> e-mail: gurin@bsu.by

<sup>b</sup> e-mail: vitalii@ccmc.unam.mx

<sup>c</sup> e-mail: alex@fhi-berlin.mpg.de

interaction with the skeleton. Non-active metals (like Ag, Cu, Au) do not bond with the matrix that results in the metal atom aggregation rather than formation of any silicate compounds.

## 2 Description of samples and measurements

The first type of matrices used for incorporation of metals was mordenites with variable  $\text{SiO}_2/\text{Al}_2\text{O}_3$  molar ratio (MR) from 10 to 206, supplied and characterized by TOSOH Co., Japan. Surface area  $S_{BET}$  and micropore volume  $V_\Sigma$  were determined by high-resolution nitrogen adsorption measurements on an Autosorb-1 Quantachrome equipment at  $10^6 < p/p_o < 1$ .  $S_{BET}$  was varied in the range 300–500  $\text{m}^2/\text{g}$  for mordenites,  $V_\Sigma$  does the range 0.2–0.3  $\text{cm}^3/\text{g}$ . Ion exchange was carried out from  $\text{Cu}(\text{NO}_3)_2$  aqueous solution. The reduction heat treatment was done in a hydrogen flow at different temperatures (20–450 °C, 4 h), and the formation of reduced species was recorded by diffuse reflectance spectroscopy (DRS) in the UV-visible range with a Varian Cary 300 device.

The second type of materials was the silica xerogels prepared by the conventional sol-gel sequence [8] using acid-catalyzed hydrolysis of tetraethoxysilane in water-alcohol mixture. The precursor sol was pH-adjusted (6.5) by ammonia, mixed with aerosil ( $\text{SiO}_2$  with size of particles about 10 nm), centrifuged and gelled in plastic pre-forms. Obtained samples were dried and heated up to 600 °C to remove organic residuals and major part of water.  $S_{BET}$  of the xerogels was determined to be 316  $\text{m}^2/\text{g}$ . They were impregnated with 0.1 N alcohol solutions of  $\text{Cu}(\text{NO}_3)_2$ , dried and heated in hydrogen atmosphere at different temperatures. The reduction products were investigated with UV-vis spectroscopy in the transmittance mode for the samples about 1 mm thickness using a Spekord M40 device.

The samples under study are denoted as Cu followed by Mor and MR value for mordenites or XG for silica xerogels and temperature of reduction in °C, *e.g.* CuMor15-150 or CuXG-200.

Foam Cu was used as received, while 0.5–10 wt% of Cu on supports ( $\gamma\text{-Al}_2\text{O}_3$  and pumice) were prepared through impregnation of supports with  $\text{Cu}(\text{NO}_3)_2$  solution followed by calcination at 600 °C for 4 h. Cu/pumice and Cu-foam samples were treated in the industrial process of partial oxidation of methanol in a flow catalytic apparatus at 650 °C for 36 h.

## 3 Experimental results and interpretation

### 3.1 Optical absorption of reduced Cu-mordenites

The absorption band peaked at  $\lambda \sim 550\text{--}600$  nm is present (Fig. 1a) in the spectra of all the samples besides CuMor15. It can be assigned to the plasmon resonance of copper nanoparticles and very known for copper in different media. Because of their size, exceeding diameters

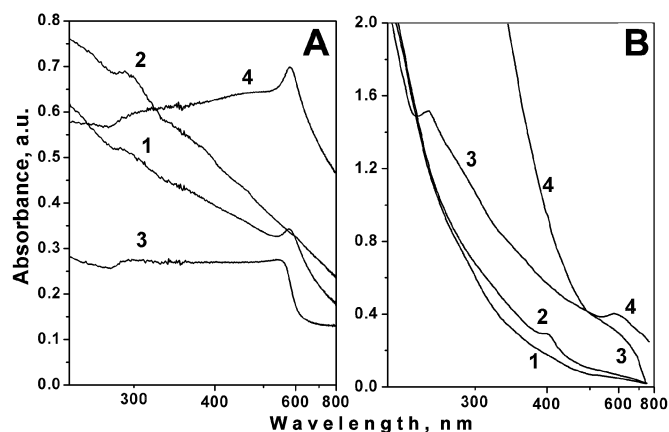


**Fig. 1.** (A) Absorption spectra of reduced CuMor samples: 1 – CuMor10-150; 2 – CuMor15-150; 3 – CuMor30-450; 4 – CuMor206-450 and (B) reduced CuXG samples: 1 – CuXG-100; 2 – CuXG-150; 3 – CuXG-300; 4 – CuXG-400. The over-scaling of some spectra is due too the limit of the spectral device used for absorption (optical density) > 2.

of regular mordenite channels, these particles may not be localized within the intracrystalline mordenite channels. They can be at surface of microcrystals or at the specific sites inside of the mordenite matrix like cleaved areas, defects, uneven surface, etc.

The short-wave bands,  $\lambda < 300$  nm, are the next feature observed for Cu-mordenite samples. Its assignment to small copper clusters is quite probable, in particular, for CuMor15 case (curve 2 in Fig. 1a). In the other Cu-mordenite samples it can interfere with interband transitions in metal copper, however, CuMor15 does not contain the metal particles those could be evidenced with the plasmon resonance band. The latter in this series of samples is governed by the logic of more favorable nanoparticles formation for the high MR and high temperatures. The shape of this band is shown to be very sensitive to MR and reduction temperature.

Thus, among the reduced products of  $\text{Cu}^{2+}$  in mordenite the few-atomic copper clusters can appear under the mild reduction conditions. The regular channels in mordenite crystal structure can incorporate such clusters with appropriate size to fit the channels geometry. However, the data on direct assignment are rather disputable, and we can only note that the short-wave bands in the optical absorption were interpreted as  $\text{Cu}_n$  species in different media [9–11].

### 3.2 Optical absorption of reduced Cu-silica xerogels

Copper reduced in the xerogels reveals different behavior as compared with that in mordenite. The plasmon resonance band appears at the higher reduction temperatures as the rather broad maximum (400 °C) or the poorly developed shoulder (300 °C). Taking into account the familiar position of the plasmon resonance for copper nanoparticles and the simulation made by us recently for copper in

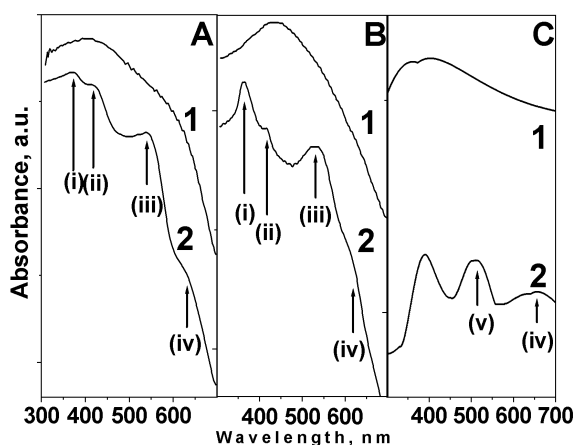


**Fig. 2.** DRS spectra of Cu/pumice (A), Cu-foam (B) and Cu/ $\gamma$ -Al<sub>2</sub>O<sub>3</sub> catalysts (C). Curves 1 and 2 in (A, B) are for fresh and the catalyst after run, respectively; curves 1 and 2 in (C) corresponds to 10wt% and 0.5wt% of Cu, respectively. Arrows mark the positions of Cu–O–Cu (i), O–Cu–O (ii), Cu nanoparticles (iii), Cu<sup>2+</sup> (iv) and CuAl<sub>2</sub>O<sub>4</sub> (v) bands.

mordenite [12], one can conclude that at the temperature about 300 °C the nanoparticles in the size range 1–2 nm are formed. The higher reduction temperatures can result in growth of the particles. However, at the lower temperatures, starting from 150 °C, the maxima corresponding to other reduced species appear: (1) peaked at 400 nm (curve 2, Fig. 1b) and (2) peaked at 255 nm (curve 3, Fig. 1b). The over-scaling in the spectrum corresponding to 300 °C reduction does not admit to say about possible appearance of the similar short-wavelength maximum in this case. Thus, the reduction of copper in xerogels begins at the higher temperatures than in mordenites, and species in the size range lower than nanoparticles generated the plasmon resonance band are observed. Their assignment to the few-atomic copper clusters is also probable (as well as in the mordenite, *e.g.* CuMor15 sample). The band about  $\lambda = 300$  nm (observed both in mordenites and silica xerogels) can be prescribed to some small Cu clusters, and the band at 410 nm (in silica xerogels only) is proposed to be related to the clusters Cu<sub>*n*</sub><sup>*x+*</sup>,  $n < 5$ ,  $x < 3$  [9–11] produced in solutions. The interpretation of the short-wavelength for the reduced copper species can be supported by theoretical calculations [13] those indicate that for relatively stable isomers of Cu<sub>*n*</sub> with  $n = 6–10$  absorption bands can exist at  $\lambda < 400$  nm, but they are strongly dependent on charge of clusters and geometry.

### 3.3 Reduced copper in catalysts

UV-visible spectra of fresh-prepared Cu/pumice and foam-Cu samples display only unstructured absorption corresponding to large metal particles (Fig. 2). Cu/pumice sample is in the form of big particles (> 1000 nm). These aggregates do not have discrete signals in UV-vis range. After the catalyst run in the reactor the spectroscopic pattern of the catalysts was changed noticeably. Electron

microscopy for this transformation revealed that part of big particles of copper was aggregated into larger ones (> 3000 nm). However, 40–50% of the support surface was not covered by the aggregates and contained highly dispersed metal. These copper nanoparticles display a number of characteristic signals in UV-vis range.

In the spectrum of Cu/pumice catalyst the noticeable signals at the wavelengths 370, 425, 550 nm and wide absorption in the 620–660 nm range are observed (Fig. 2a). According to [14–17] the first two signals can belong to O–Cu–O (i) and Cu–O–Cu (ii) complexes (charge transfer bands). Absorption at 620–660 nm (iv) is attributed to electron *d*–*d* transitions of Cu<sup>2+</sup> in distorted octahedral surrounding by oxygen in CuO particles. Absorption bands in the range of 520–540 nm (v) are close to the copper plasmon resonance, but evidently it has the different nature and can be related to the possible binary oxide phase CuAl<sub>2</sub>O<sub>4</sub> [16]. This band is clearly seen for the 0.5 wt% of copper in  $\gamma$ -alumina sample (Fig. 2c). In pumice this signal can belong more probably to the plasmon resonance (iii) of Cu nanoparticles like to the case of foam-copper (Fig. 2b) (that does not contain alumina). Thus, the prolonged run of the sample in catalytic reactor favours the formation of oxidized copper states and the metal nanoparticles.

At high metal percentage (10 wt% of Cu) Cu/ $\gamma$ -Al<sub>2</sub>O<sub>3</sub> samples do not have any discrete absorption bands in the spectra, only the unstructured rise is observed (Fig. 2c). According to electron microscopy data the average size of the metal particle in this sample is 150–200 nm, much larger than at the lower metal percentage.

Unexpected signals are observed in the spectra of exhaust foam-copper catalyst and Cu/pumice, namely, two pronounced bands at 365 nm (i) (O–Cu–O) and 550 nm (iii) (Fig. 2b) and the weaker ones at 420 (ii) and 620 nm (iv). They indicate significant changes in the state of copper surface as the result of catalytic runs. Both oxidized and reduced states are created due to interaction with reaction mixture. Copper nanoparticles are produced on the surface of bulk metal, perhaps, from surface oxide layer which is not reduced completely since the contact with air remains. The system requires further in situ studies monitoring this variable composition. Thus, the catalytic reaction accompanied by oxidation-reduction cycles of metallic Cu favours the formation of small metal particles.

## 4 Conclusions

The properties of reduced copper species incorporated in mordenites, amorphous silica xerogels and catalyst supports are definitely influenced by matrix structure, MR value in mordenite and reduction temperature. Metal particles exhibiting the plasmon resonance band are formed under the higher reduction temperatures in different matrices. Their appearance has complicated dependence on MR in mordenites. Small copper clusters were proposed to be responsible for the short-wavelength absorption bands in the xerogels and mordenite with certain MR value.

The clusters can be produced under mild conditions. The spectroscopic features of copper in catalyst supports coincide with those in mordenites and silica xerogels only in appearance the plasmon resonance band. On the other hand, these supports contain noticeable amount of the oxidized states. During the catalytic process a part of highly dispersed copper is increased, but the oxidized states remain also.

Thanks are given to E. Aparicio, E. Flores, J.A. Peralta, C. Gonzalez Sanchez for the precious technical support. The research reported in this paper was supported by CONACYT, Mexico, through Grant No. 32118-E and Russian Federation President grant No. 02-15-99360.

## References

1. *Atomic clusters and nanoparticles*, edited by C. Guet, P. Hobza, F. Spiegelman, F. David, NATO Advanced Study Institute, Les Houches, Session 73 (EDP Sciences, Springer-Verlag, 2001)
2. P. Jena, S.N. Khanna, B.K. Rao, *J. Cluster Sci.* **12**, 443 (2001)
3. J.D. Aiken III, R.G. Finke, *J. Mol. Catal. A* **145**, 1 (1999)
4. A.N. Pestryakov, V.V. Lunin, A.N. Devochkin, L.A. Petrov, N.E. Bogdanchikova, V.P. Petranovskii, *Appl. Catal. A* **227**, 125 (2002)
5. A.N. Pestryakov, A.A. Davydov, *Appl. Surf. Sci.* **103**, 479 (1996)
6. J.K. Walker, *Formaldehyde*, 3rd edn. (Reinhold, New York, 1964)
7. A.N. Pestryakov, A.A. Davydov, P.G. Tsyrunnikov, *Prepr. Am. Chem. Soc., Div. Pet. Chem.* **41**, 96 (1996)
8. L.L. Hench, J.K. West, *Chem. Rev.* **90**, 33 (1990)
9. B.G. Ershov, E. Janata, A. Henglein, *Radiat. Phys. Chem.* **39**, 123 (1992)
10. J. Khatouri, M. Mostafavi, J. Amblard, J. Belloni, *Chem. Phys. Lett.* **191**, 351 (1992)
11. G.A. Ozin, S. Mitchell, D.F. McIntosh, S.M. Mattar, J.J. Garcia-Prieto, *Phys. Chem.* **87**, 4665 (1983)
12. V. Petranovskii, V. Gurin, N. Bogdanchikova, A. Licea-Claverie, Y. Sugi, E. Stoyanov, *Mater. Sci. Eng. A* **332**, 174 (2002)
13. J.A. Alonso, *Chem. Rev.* **100**, 637 (2000)
14. S.F. Tikhov, E.A. Paukshtis, V.A. Sadykov, *Kinet. Catal.* **30**, 869 (1989)
15. G.A. Dergaleva, N.A. Pakhomov, V. Bendurin, V. Anufrienko, *Kinet. Catal.* **32**, 490 (1991)
16. M. Arai, S. Nishiyama, S. Tsuruya, M. Masai, *J. Chem. Soc., Faraday Trans.* **92**, 2631 (1996)
17. M.C. Marion, E. Garbovski, M. Primet, *J. Chem. Soc. Faraday Trans.* **86**, 3027 (1990)